PCCP

Anion-π interaction with alkenes: persistent complexes vs irreversible reactions of anions with tetracyanoethylene

Journal:	*Physical Chemistry Chemical Physics*
Manuscript ID	CP-ART-06-2024-002573.R2
Article Type:	Paper
Date Submitted by the Author:	18-Jul-2024
Complete List of Authors:	Odubo, Favour E.; Ball State University Muthuramesh, Snehashree; Ball State University Zeller, Matthias; Purdue University Rosokha, Sergiy; Ball State University

ARTICLE

Anion-π interaction with alkenes: persistent complexes vs irreversible reactions of anions with tetracyanoethylene

Received 00th January 20xx,
Accepted 00th January 20xx

DOI: 10.1039/x0xx00000x

Favour E. Odubo,[a] Snehashree Muthuramesh,[a] Matthias Zeller,[b] and Sergiy V. Rosokha*[a]

The interaction of the tetracyanoethylene (TCNE) π-acceptor with oxo- and fluoro-anions (BF_4^-, PF_6^-, ClO_4^-, NO_3^-) led to the formation of anion-π complexes in which these polyatomic anions were located over the face of alkenes, with multiple contacts being shorter than the van der Waals separations. The anion-π associations of TCNE with halides were delimited by the electron-donor strengths and nucleophilicity of the anions. Specifically, while bromides formed persistent anion-π associations with TCNE in the solid state and in solutions, only transient anion-π complexes with iodides and chlorides were observed. In the case of iodide (strong 1e reducing agent), the formation of anion-π complexes was followed by the reduction of the π-acceptor to the $TCNE^{\bullet-}$ anion-radical. The interaction of TCNE with Cl^- (and F^-) anions (which are better nucleophiles in the aprotic solvents) led to the formation of 1,1,2,3,3-pentacyanoprop-2-en-1-ide anions. Thermodynamics, UV-Vis spectra, and structures, as well as contributions of electrostatics, orbital interactions, and dispersion to the interaction energies in the complexes of TCNE with various anions were closely related to the characteristics of the corresponding associations with the aromatic and p-benzoquinone acceptors. This points out the general equivalence of the interactions in the anion-π complexes with different π-acceptors and the critical role of the nature of the anions in these bindings.

Introduction

Following seminal theoretical articles showing the attraction of anions to electron-deficient π-systems (e.g., triazine or perfluorobenzene) in 2002,[1-3] anion-π interactions became one of the central topics of supramolecular chemistry.[4-6] These computational works were followed by experimental verifications of anion-π binding[7-11] demonstration of its high potential for anion recognition and transport, catalysis, and other applications.[12-16] The detailed accounts of the development in this area is described in several excellent reviews.[5,6,11,12] The main attention in the studies of this counter-intuitive interaction was directed toward the bonding between anions and aromatic molecules with electron-withdrawing substituents (e.g., halogens, nitro or cyano groups).[1-6] There are also several publications describing the associations of anions with the faces of cyano- and/or halogen-substituted benzoquinones, and studies of attractive interaction of lone pairs with the π* antibonding orbitals of carbonyl groups.[17-19] Nevertheless, the data about binding between anions and the simplest π-systems, molecules containing one C=C double bond, is scarce.[9,20,21] This raises the question about the nature and characteristics of such an unusual bonding, and its relation to previously described anion-π interactions.

Similarly to the aromatic and benzoquinone molecules, the possibility of the attraction of anions to alkenes depends on the presence of the electron-withdrawing substituents which decrease electron density over the face of the π-system. Thus, to explore the anion-π interaction involving such species, we turned to a well-known olefinic π-acceptor , tetracyanoethylene (TCNE, Figure 1).[22] The withdrawal of the electron density from the ethylene fragment by the four cyano-groups results in a positive electrostatic potential over the face of this essentially planar molecule (Figure 1).[21] This suggests an attraction of anions to this area. Indeed, the crystallographic literature contains X-ray structures of associations of TCNE with bromide, thiocyanate, and tetrahalometallates.[9,20,21] Yet, there are essentially no experimental or computational data on the thermodynamics and spectral properties of these complexes in solutions, about the bonding of TCNE with other anions, or the nature and main components of this bonding interaction.

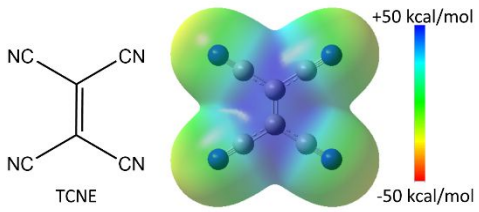

Figure 1. Structure, acronym and surface electrostatic potential of TCNE (at 0.001 a.u. electron density)

[a] Department of Chemistry, Ball State University, Muncie, Indiana, 47306, USA
[b] Department of Chemistry, Purdue University, West Lafayette, Indiana, 47907, USA

† Electronic Supplementary Information (ESI) available: X-ray structures and details of the X-ray crystallographic analysis, results of the UV-Vis measurements and details of the treatment of the spectral data, quantum theory of atoms in molecules and energy decomposition analyses data, energies and atomic coordinates of the optimized complexes. See DOI: 10.1039/x0xx00000x

In the current work, we examined the interaction of TCNE with various anions in the solid state and solutions, as well as scrutinized their properties using computational methods. Our goal was to compare anion-π complexes of olefinic π-acceptors with those involving aromatic (e.g., tetracyanopyrazine) or p-benzoquinone (e.g., tetrafluoro-p-benzoquinone) acceptors, and to clarify similarities and distinctions (if any) in the characteristics of the different types of complexes.

Besides the π-acceptors, characteristics of the anion-π complexes are determined by the nature of the anions. We have shown earlier that while the overall strength of interaction is similar, the contributions of the electrostatics, dispersion, and orbital interactions were very different for complexes of aromatic or p-benzoquinone acceptors with polyatomic fluoro- or oxoanions as compared to those with monoatomic halide anions.[23] These distinctions manifested in different experimental UV-Vis spectral properties of the complexes. Thus, to verify the generality of these observations, we examined herein interaction of TCNE with anions with different structural and electronic characteristics. They include monoatomic (halides), linear (thiocyanate), planar (NO_3^-), tetrahedral (BF_4^- and ClO_4^-), and octahedral (PF_6^-) species. Besides, these anions allow to compare properties of complexes with nucleophilic (and reducing) species with those of inert weakly-coordinating and difficult to oxidize oxo- and fluoroanions.

Indeed, many electron-rich anionic species, in particular halides, are good reducing agents and nucleophiles. On the other hand, the presence of four cyano-substituents makes TCNE molecule a strong π-acceptor with a reduction potential of 0.17 V vs SCE in acetonitrile.[24] As such, it might be easily reduced by various chemical or electrochemical methods. In fact, the reaction of TCNE with iodide was one of the earliest and the most common methods of preparation of the anion-radicals of this π-acceptor.[25-27] These persistent anion-radicals played a central role in the development of the molecular magnets and the concept of multicenter (pancake) bonding.[28] Also, the interaction of TCNE with various nucleophiles in the presence of water resulted in the formation of polycyano-substituted anionic species.[29,30] The σ-bonded complexes of anions with TCNE were suggested as the intermediates of these transformations.[30] As such, another goal of the current work was to establish boundaries between the reversible formation of the anion-π complexes with TCNE and the irreversible chemical processes, in particular 1e-reduction or nucleophilic addition, of this π-acceptor.

Results and discussion

1. X-ray crystallography of the anion-π associations and products of reactions of TCNE with anions.

Co-crystallization of TCNE with $(Pr_4N)NO_3$ produced 1D stacks of alternating π-acceptor and anion moieties (Figure 2A). Within these stacks (which are surrounded by the tetrapropylammonium counter-ions), NO_3^- anions were nested between two TCNE molecules. The latter are tilted relative to each other by about 65°, but every other TCNE moiety is parallel (similar to the observed earlier for anion-π bonded stacks with aromatic tetracyanopyrazine acceptors).[20]

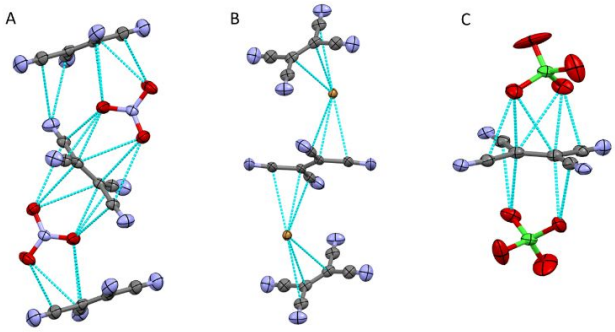

Figure 2. Fragments of the crystal structures showing chains of the alternating anions and π-acceptors in $(Pr_4N)NO_3$·TCNE (A), $(Pr_4N)NO_3$·TCNE (B), and the 2:1 complex of $((Pr_4N)ClO_4)_2$·TCNE (C). Note that tetrapropylammonium counter-cations are omitted for clarity. The blue lines show contacts shorter than the van der Waals separations of the interacting atoms (3.22 Å and 3.55 Å for C/O and C/Br pairs, respectively).

Co-crystals of TCNE with methyltriphenylphosphonium bromide comprised analogous alternating chains of TCNE and anions (Figure 2B). The bromide anions were located close to the top of the sp^2 carbons, with Br-C=C angles of 111.7 and 83.0 deg. Both TCNE/NO_3^- and TCNE/Br^- chains comprise multiple contacts between anions and π-acceptors which are shorter than the sums of the van der Waals radii of the corresponding atoms. Selected interatomic distances in these co-crystals are listed in Table 1.

Co-crystallization of TCNE with tetrapropylammonium perchlorate or tetrafluoroborate salts produced 1:2 solid-state complexes in which two anions are arranged on both sides of the π-acceptors (Figure 2C and Figure S1 in the Supporting Information, note that similar arrangements are observed for $((Pr_4N)PF_6)_2$·TCNE, but ions and TCNE moieties are disordered in these co-crystals). While stoichiometry and the architectures of these co-crystals are different from those formed by TCNE with Br^- or NO_3^-, they share the same principal feature. Specifically, the anions are located over the faces of the TCNE molecules, and they show multiple contacts that are shorter than the van der Waals separations (Table 1). This indicates a strong attraction of anions to the π-acceptor. To verify this suggestion, we carried out QTAIM and NCI analyses of these solid-state associations.

A quantum theory of atoms in molecules (QTAIM) analysis[31] revealed bond paths between anions and TCNE in each solid-state association (Figure 3 and Figure S2 in the Supporting Information).

Table 1. Characteristics of the selected short contacts in the co-crystals of TCNE with various anion.

Anion	Contact	$d_{X\cdots C}$, Å	$\rho(\mathbf{r})$, a.u.	$H(\mathbf{r})$, a.u.	-ΔE,[a] kcal/mol
NO_3^-	O-$C_{C=C}$	2.713	0.0102	0.0021	2.1
	O-$C_{C\equiv N}$	2.813	0.0090	0.0017	1.8
Br^-	Br-$C_{C=C}$	3.343	0.0109	0.0008	1.9
	Br-$C_{C=C}$	3.350	0.0103	0.0009	1.7
ClO_4^-	O-$C_{C\equiv N}$	2.798	0.0122	0.0018	2.6
	O-$C_{C=C}$	2.860	0.0111	0.0016	2.1
BF_4^-	O-$C_{C=C}$	2.841	0.0160	0.0021	3.5
	O-$C_{C\equiv N}$	2.902	0.0070	0.0012	1.2

a) Calculated based on the energy density, E = ½V(r).[32] b) Angle between I-C bond and perpendicular to the pyridinium plane.

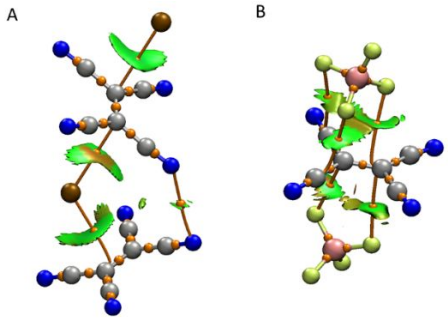

Figure 3. QTAIM and NCI analyses of the solid-state $(MePh_3P)Br{\cdot}TCNE$ (A) and $((Pr_4N)BF_4)_2{\cdot}TCNE$ (B) associations (using atomic coordinates extracted from the X-ray structures). Orange lines and orange spheres show bond paths and BCPs and blue-green areas indicate bonding interactions (note that calculations were done using dianinic fragments shown in this figure).

Characteristics of the (3,-1) bond critical points (BCPs) along these bond paths are listed in Table 1 and Table S1 in the Supporting Information. The electron densities at BCPs for all associations are close to 0.01 a.u. These values are typical for moderately strong non-covalent interactions.[33] The very small positive values of energy density at these points indicate a predominantly electrostatic nature of these bondings. The energies of these interactions (estimated using values of the potential energy density at BCPs[32]) were around 2 kcal/mol. The NCI analysis[34] showed blue-green areas around each BCP which further confirmed a relatively weak attractive interaction between anions and TCNE.

While the interaction of TCNE with salts of fluoro-/oxo-anions, and bromide led to the formation of anion-π associations, crystallization with alkylammonium chloride or fluoride salts produced 1,1,2,3,3-pentacyanoprop-2-en-1-ide (abbreviated hereinafter as PCP^-) anions (Figure S3 in the Supporting Information).‡ Also, reactions of TCNE with alkylammonium salts of iodide resulted previously in the reduction of TCNE and crystallization of the salts of $TCNE^{-\bullet}$ anion-radicals.[26] Thus, besides the well-known reduction of TCNE by iodide (due to the low redox potentials for the I_3^-/I^- pair of 0.06 V vs SCE[35]) the formation of the persistent anion-π complexes of TCNE with halides is limited by the nucleophilicity of anions (since chloride and fluoride are better nucleophiles in aprotic solvents as compared to the bromide[36]). To further elucidate the interactions between TCNE and various anions, we turned to their measurements of their properties in solution.

3.2. UV-Vis study of the interaction of anions with TCNE

The addition of Br^- anions to the solutions of TCNE in acetonitrile or dichloromethane led to the appearance of a new absorption band in the UV-Vis spectra (with λ_{max} at 469 nm and 460 nm in CH_2Cl_2 and CH_3CN, respectively) which was not present in the spectra of the individual reactants (Figure 4 and Figure S4 in the Supporting Information). In solutions with a constant concentration of TCNE, the intensity of this band increased with the rise of the concentration of Br^- anions. This dependence was well-fit to the binding isotherm of a 1:1 complex between TCNE and Br^-:

$$TCNE + Br^- \rightleftarrows [TCNE{\cdot}Br^-] \qquad (1)$$

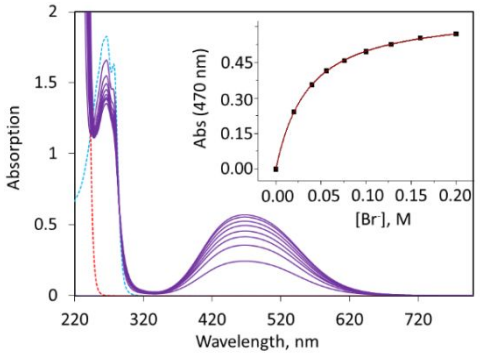

Figure 4. Spectra of solutions with variable concentrations (from 0.02 to 0.2 M) of $(Bu_4N)Br$ and a constant concentration (1.5 mM) of TCNE in CH_2Cl_2 (purple lines). Dashed red and blue lines show spectra of the solutions of individual $(Pr_4N)Br$ and TCNE, respectively. Insert: Dependence of the intensity of absorption at 470 nm on the concentration of Br^- (the solid line shows a fit of the data to a 1:1 binding isotherm).

In contrast to Br^-, an addition of I^- or Cl^- anions to the solutions of TCNE resulted only in transient formation of anion-π complexes. In particular, the spectrum of the solution obtained upon the addition of the iodide to the solution of TCNE in dichloromethane at 20 °C resulted in immediate formation of a spectrum that represented a superposition of the absorption of $TCNE^{-\bullet}$ anion-radical (band at 425 nm with the characteristic vibrational splitting[27]) and I_3^- anions (strong band with a maxima at 360 and 295 nm[17]). This indicates the fast reduction of TCNE by iodide with formation of $TCNE^{-\bullet}$ and I_3^- (this reaction is a common method of preparation of TCNE anion – radicals.[25-27]) However, when the solutions of TCNE and I^- were mixed at -85 °C, a broad absorption band appeared at 650 nm (Figure 5). DFT calculations§ and Mulliken correlations (vide infra) indicated that this band represents absorption of a $TCNE{\cdot}I^-$ complex. Warming of this solution led to fast decrease of the disappearance of this band and appearance of the bands of $TCNE^{-\bullet}$ and I_3^-. It suggests that the anion-π complex of TCNE with iodide represent an intermediate in the formation of $TCNE^{-\bullet}$ anion-radical, i.e.

$$2TCNE + 3I^- \rightleftarrows 2[TCNE{\cdot}I^-] + I^- \rightarrow 2TCNE^{-\bullet} + I_3^- \qquad (2)$$

The addition of chloride to the solution of TCNE resulted in the appearance of a broad absorption band at 408 nm (Figure 6).

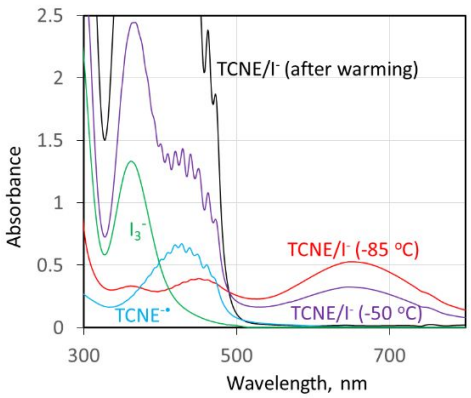

Figure 5. Spectrum (red line) formed upon mixing of equimolar (1.0 mM) solutions of TCNE and $(Bu_4N)I$ in CH_2Cl_2 at -85 °C. Violet and black lines show spectra measured upon warming of this solution to -50 °C and to +20°C. Blue and green lines show spectra of the individual $TCNE^{-\bullet}$ and I_3^- ions, respectively.

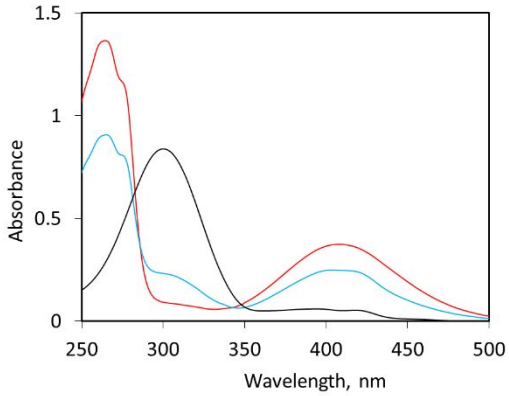

Figure 6. Spectra of the solutions containing TCNE and Bu_4NCl in dichloromethane measured at 22 °C immediately after mixing (red line showing band of anion-π complex at 410 nm), after 10 min (blue line), and after 24 h (black line showing band of PCP^- at 310 nm).

The intensity of this band decreased with time and a new absorption band with a maximum at 301 nm appeared (see time-dependent spectra in Figure S5 in the Supporting Information, note that mixing of the solution of TCNE and Cl^- in acetonitrile led to immediate appearance of the analogous band at 300 nm). TD DFT calculations of the TCNE·Cl^- (anion-π) complex§ and 1,1,2,3,3-pentacyanoprop-2-en-1-ide anions, PCP^- (which were obtained in the crystalline state from the solutions containing TCNE and chloride) produced absorption bands which were reasonably close to the bands at 410 and 310 nm, respectively. It suggests that these bands represent anion-π complex and PCP^- anions. Furthermore**,** the absorption band energies of the complexes of TCNE with halides (and with thiocyanate[21]) follow the same Mulliken correlation[37] with the difference of the redox-potentials of the interacting species (Figure 7) as the reported earlier bands of the halides and thiocyanate complexes with aromatic and benzoquinone acceptors.[17, 38] This supports assignments of the transient absorption bands measured with I^- and Cl^- anions and suggests a close relationship between complexes with different π-acceptors.

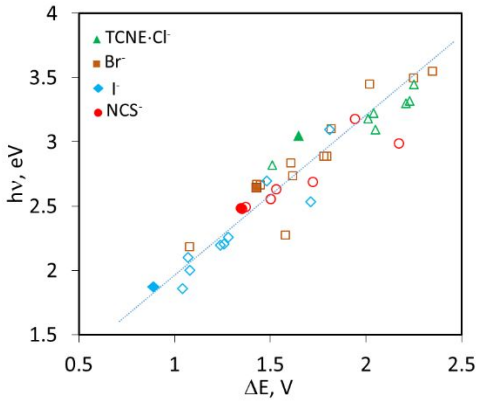

Figure 7. Correlation between energies of the absorption bands and the difference of the redox potentials of the reactants in the complexes of Cl^- (green triangles), Br^- (brown square), I^- (blue rhombuses), and NCS^- (red circles) with different π-acceptors. The filled symbols indicate complexes with TCNE, and open symbols present the data with aromatic and p-benzoquinone π-acceptors[17] (see Table S2 in the Supporting Information for the details).

In contrast to halides, addition of oxo- or fluoroanions to the solutions of TCNE did not produce new absorption bands in the UV-Vis range (Figure 8 and Figures S6 in the Supporting Information). The close inspections of the spectra of these solutions revealed, however, that their absorptions deviate from that of TCNE itself. Subtraction of the latter from the spectra of mixtures showed that the addition of the oxo- or fluoroanions results in a small increase or decrease of the absorption in various regions of the TCNE band. Importantly, these differential absorptions could be fitted with 1:1 binding isotherms (Figures S6 - S9 in the Supporting Information) similar to those used for fitting of the spectra in solutions with bromide .

The values of the *apparent* equilibria constants K of 8 M^{-1} to 80 M^{-1} which were obtained from such the fitting of the UV-Vis data measured in dichloromethane are listed in Table S3 in the Supporting Information. For comparison, Table S3 includes also the characteristics of the related anion-π complexes with the aromatic tetracyanopyrazine (TCP), tetrafluoro- (pFA) or dichlorodicyano-p-benzoquinone (DDQ) π-acceptors which were reported earlier.[23] It should be stressed that due to the variation of ionic strength in the series of the solutions that were used for the UV-Vis measurements, the values of K do not represent true equilibrium constants.[38] Still, the fact that the values obtained for the complexes of TCNE are in the same range as those measured in an analogous way with aromatic and p-benzoquinone molecules indicates a comparable strength of the interaction with different types of π-acceptors. Also, in agreement with the calculated solvent dependence of the binding energies (Figure S10 and Table S4 in the Supporting Information) and our previous studies of complexes with p-benzoquinones,[23] the apparent constant of the formation of the complex of TCNE with Br^- measured in acetonitrile (7.0 M^{-1}) was lower than that in dichloromethane (31 M^{-1}). The spectral changes occurring upon the addition of PF_6^{--}, BF_4^-, and ClO_4^- to TCNE in acetonitrile were too small for measurements of formation constants of the corresponding complexes in this solvent.

Overall, UV-Vis measurements showed that the spectral features and apparent formation constants of the complexes of TCNE with various types of anions are similar to those reported earlier for the analogous associations with the aromatic and p-benzoquinone π-acceptors.[23] To examine the nature of the anion-π interactions in the complexes with TCNE, we turned to computational analyses.

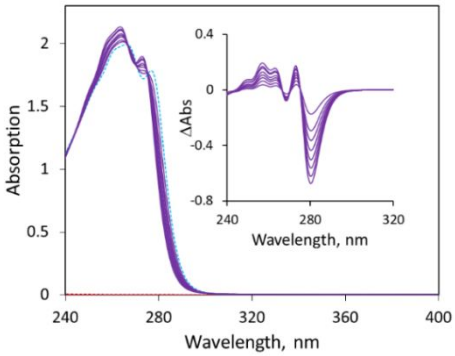

Figure 8. Spectra of the solutions (purple lines) containing variable (20 to 200 mM) concentrations of $(Bu_4N)BF_4$ and a constant (1.5 mM) concentration of TCNE in CH_2Cl_2. Dashed red and blue lines show spectra of the individual solutions of $(Pr_4N)BF_4$ and TCNE, respectively. Insert: Differential spectra of the solution which were obtained by the subtraction of the absorption of individual components from the absorption of the mixture.

3. Computational analysis of the interaction of TCNE with anions.

The structures resulting from M06-2X/def2-TZVPP optimization of the complexes of TCNE with various anions together with the results of their QTAIM and NCI analyses are illustrated in Figure 9. In general, the arrangements of the anions and π-acceptors in the optimized 1:1 complexes were consistent with the structures of the solid-state associations obtained from the X-ray crystallographic analysis (although the latter represented 1D chains with 2:2 anion-π-acceptor contacts or 2:1 complexes). In particular, oxo- and fluoroanions in these complexes were located over the C=C double bond. The calculated complex with nitrate, however, comprised essentially co-planar NO_3^- and TCNE moieties (while the NO_3^- plane is close to perpendicular to the TCNE molecules and shows close O…C contacts on both its sides in the X-ray structure). All these complexes show contacts between the anions and TCNE which are shorter than their van der Waals separations (Table 2), and these interatomic distances are consistent with the values measured in the solid-state.

Optimizations of the complexes of TCNE with Cl^-, Br^- and I^- anions produced structures similar to those obtained by X-ray analysis for the complex of TCNE with bromide. It should be noted, however, that the Br…C separation in the optimized complex is about 0.4 Å shorter than in the experimental X-ray structure in Table 1. Such a difference is probably related to the fact that the solid-state associations represent 1D chains in which each bromide interacts with two TCNE molecules and vice versa, as well as stronger effects of counter-ions and crystals forces on the location of these monoatomic anions. The halide anions were located near the top of one of the sp^2 carbons. The X-C=C angles (109.2, 108.1 and 107.2° for optimized pairs with Cl^-, Br^-, and I^-, respectively) are close to the value characteristic for the Burgi-Dunitz trajectory for the nucleophilic attack on an sp^2 carbon.[39] In comparison, the optimizations of the systems with the stronger nucleophiles, F^- and N_3^- (the latter was chosen for the comparison with NCS^-) produced σ-bonded complexes.

The binding energies of the anion to TCNE in all calculated anion-π complexes are in the 9±3 kcal/mol range. Similar values were reported earlier for the complexes of the same anions with aromatic and p-benzoquinone acceptors.[23] The binding of anions in the σ-bonded complexes with F^- and N_3^- are about three times stronger.

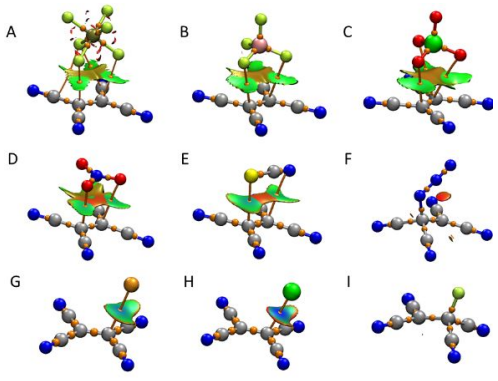

Figure 9. Superposition of the results of QTAIM and NCI analyses onto the optimized structures of the complexes of TCNE with PF_6^- (A), BF_4^- (B), ClO_4^- (C) NO_3^- (D), NCS^- (E) N_3^- (F), Br^- (G), Cl^- (H) and F^- (I). The bond paths and critical (3, -1) points (from QTAIM) are shown as orange lines and spheres, and blue-green areas (from NCI) indicate bonding interactions.

Table 2. Characteristics of the optimized anion-π complexes

X^-	E, kcal/mol	$d_{X\ldots C}$,[a] Å	λ_{max}, nm	Δq,[b] e	$d_{C=C}$, Å
PF_6^-	-7.3	2.780	262	0.02	1.346
BF_4^-	-8.4	2.754	262	0.02	1.346
ClO_4^-	-8.5	2.852	287	0.03	1.347
NO_3^-	-9.8	2.730	301	0.08	1.349
Cl^-	-9.7	2.694	390	0.20	1.357
Br^-	-7.9	2.957	461	0.16	1.355
I^-	-6.6	3.202	560	0.17	1.355
NCS^-	-11.8	2.841	448	0.22	1.357
N_3^-	-24.5	1.529	293	0.88	1.490
F^-	-37.6	1.418	230	0.65	1.465

a) The shortest contact between the anion and TCNE. b) Charge-transfer from the anion to the TCNE moiety. c) The C=C bond length.

The QTAIM analysis showed bond paths and BCPs between anions and TCNE moieties in all calculated complexes. The energy and electron densities at BCPs (Table S5 in the Supporting Information) are similar to those in the experimental solid-state associations.

While the binding energies for the oxo- and fluoroanions were similar to those in the anion-π complexes with (pseudo-)halides, the spectral properties of these complexes obtained via TD DFT calculations were different. The optimized anion-π complexes with (pseudo-)halides show intense absorption bands in the visible range. Their energies are close to those measured experimentally, and they decrease with the increase of electron-donor abilities of the anions, which supported the charge-transfer character of these transitions (The computational analysis showed that they represent a photoinduced transfer of electrons from the highest occupied molecular orbitals, HOMOs, of the complex which were located primarily on the anions to the lowest unoccupied molecular orbitals, LUMOs, which resides mainly on TCNE). In comparison, the absorption bands in the calculated spectra of complexes with oxo- and fluoroanions are close to those of the individual TCNE acceptors. Since oxo- and fluoroanions are poor electron donors (i.e., their HOMOs are lower), the electronic transitions from the HOMOs (residing on the anions) to the LUMOs located on TCNEs overlap with the intramolecular transitions within the individual π-acceptors.

Besides the differences in the spectra, the better electron-donating properties of the (pseudo-)halide anions explain the higher ground-state n-π* charge transfer from these anions to TCNE in their anion-π complexes as compared to the value found in the complexes with the oxo- and fluoroanions (Table 2). The n-π* charge transfer led to slight (about 0.007 Å) lengthening of the C=C bond (Table 2) as compared to the bond (1.345 Å) in the optimized individual TCNE and it suggests the higher contribution of charge-transfer (molecular-orbital) interactions in the complexes with the halides.

To verify the distinctions in the interactions of TCNE with different anions, we performed an energy decomposition analysis (EDA) of these bondings using the AMS suite of programs.[40] This method decomposes the intermolecular interaction energy into electrostatic, ΔE_{elstat}, Pauli repulsion, ΔE_{Pauli}, orbital (charge-transfer) interaction, ΔE_{oi} and dispersion, ΔE_{disp}, components:[41]

$$E_{int} = E_{elstat} + E_{Pauli} + E_{oi} + E_{disp} \quad (3)$$

All these values are listed in Table S6 in the Supporting Information. Notably, while binding energies, ΔE, are rather close for all anion-π

bonded complexes, the values of E_{elstat}, ΔE_{oi}, and ΔE_{disp} depend substantially on the nature of the anions. Variations of the contributions (in %) of these components to the attractive interaction (e.g., $(\Delta E_{elstat}/(\Delta E_{elstat} + \Delta E_{oi} + \Delta E_{disp})\times 100\%$ are illustrated in Figure 10.

The data in Figure 10 show that electrostatics represents the most significant component of attractive interaction energy in all anion-π complexes. Contributions of dispersion are more than three times lower than those of electrostatics. The contributions of both ΔE_{elstat} and ΔE_{disp} are lower in the complexes with (pseudo-)halides as compared to that with the oxo- and fluoro-anions. Accordingly, orbital interactions are much stronger in the complexes with (pseudo-) halides than in the complexes with oxo- and fluoroanions. The E_{oi} values are approaching E_{ES} in the anion-π complexes with (pseudo)halides, and the contributions of different components in these associations are comparable to those in the σ-bonded complexes formed by TCNE with N_3^- and F^- anions. The substantial contribution of the molecular-orbital interaction explains the appearance of the intense charge-transfer absorption bands in the anion-π complexes with (pseudo-) halide anions.[42]

Methods

Materials. Commercially available TCNE was purified by sublimation, and tetrabutyl- or tetrapropylammonium salts of tetrafluoroborate, thiocyanate, perchlorate, hexafluorophosphate, and halides were purified by recrystallization. The methyltriphenylphosphonium salt of bromide, $(MePh_3P)Br$, was used for the preparation of single crystals without purification. Tetrapropylammonium salts of nitrate and hexafluorophosphate were prepared by neutralization of the corresponding acid with a solution of tetrapropylammonium hydroxide followed by the recrystallization from dichloromethane / hexane mixtures. Dichloromethane and acetonitrile were distilled over P_2O_5 under an argon atmosphere before use.

X-ray crystallography. Single crystals of $(Pr_4N)NO_3\cdot$TCNE, $(Pr_4N)PF_6\cdot$TCNE, $((Pr_4N)ClO_4)_2\cdot$TCNE, and $(Pr_4N)BF_4\cdot$TCNE, were prepared by cooling acetonitrile solutions containing equimolar (0.2 mmol each) quantities of TCNE and the corresponding salt from room temperature to −30 °C and keeping solutions at this temperature for several days. Single crystals obtained by similar procedures with tetrabutyl- or tetrapropylammonium salts of F^- or Cl^- anions comprised

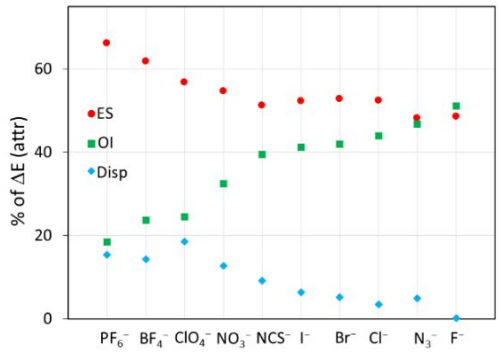

Figure 10. Contributions (in %) of ΔE_{elstat} (red circles), ΔE_{oi} (green squares), and ΔE_{disp} (blue rhombus) to the attractive interactions in the complexes of TCNE with various anions.

1,1,2,3,3-pentacyanoprop-2-en-1-ide (PCP^-) salts, $(Bu_4N)PCP$ (Figure S3) or $(Pr_4N)PCP$. To prepare crystals of $(MePh_3N)Br\cdot$TCNE, the equimolar (1.0 mmol) amounts of $(MePh_3N)Br$ and TCNE were stirred for several minutes in 3 mL of a 10:1 mixture of dichloromethane and hexane. The undissolved solid was filtered off and the solution was cooled to -30°C. Red crystals of $(MePh_3N)Br\cdot$TCNE formed after several days.

The X-ray measurements were carried out on a Bruker AXS D8 Quest diffractometer with a molybdenum radiation X-ray tube (λ = 0.71073 Å). Reflections were indexed and processed, and the files were scaled and corrected for absorption using APEX4.[43] The space groups were assigned using XPREP within the SHELXTL suite of programs, the structures were solved by dual methods using using ShelXT and refined by full-matrix least-squares against F^2 with all reflections using Shelxl2019 with the graphical interface Shelxle.[44-46] Crystallographic, data collection, and structure refinement details are listed in Table S7 in the Supporting Information. Complete crystallographic data, in CIF format, have been deposited with the Cambridge Crystallographic Data Centre. CCDC 2353176-2353181 contain the supplementary crystallographic data for this paper. These data can be obtained free of charge via www.ccdc.cam.ac.uk/data_request/cif .

UV-Vis measurements. The formation of complexes between TCNE and various anions was studied at 22 °C via UV-Vis measurements of a series of solutions with a constant (2 - 10 mM) concentration of TCNE and variable concentrations (from 0 to 0.4 M) of anions. A Dewar equipped with a quartz lens was used for the measurements at -85 °C. The apparent formation constants, *K*, were obtained (see the Supporting Information for details) via regression analysis of the differential intensities of absorption, ΔAbs (obtained by the subtraction of absorption of components from the absorption of their mixtures), for these series as described earlier.[17,23] Each point in these series represents a result of a separate measurement taken within 1-2 minutes after mixing solutions of TCNE and the salt of anion. In the case of the complexes of ClO_4^-, PF_6^-, and BF_4^- anions, the spectra of the solutions remained constant for several hours (Figure S10 in the Supporting Information). The spectra of the dichloromethane solutions of the complexes with bromide remained essentially constant for about 10-15 minutes, but small spectral changes were noticeable when such solutions were kept for several hours at room temperature (Figure S11 in the Supporting Information). These changes suggest that very slow formation of the products of nucleophilic attack (similar to that in the systems with Cl^-) and/or redox processes in solutions of TCNE with Br^- anions# (note that similar time-dependent spectral changes were observed in dichloromethane solutions of TCNE and NCS^- and NO_3^- and the rates of these processes were higher in more polar acetonitrile. The analysis of the kinetics and mechanism of these reaction requires a separate study and is beyond a scope of the current work.

In the absence of hydrogen substituents in TCNE and anions, complex formation in solutions could be measured by ^{13}C NMR. However, such measurements require a higher concentration of TCNE, than that we used for the UV-Vis measurements. Due to the limited solubility of TCNE in dichloromethane, we used more polar deuterated acetonitrile, in which formation constants of the anion-π complexes are lower.[38] Under these conditions, we observed only very small shift of the signals of C=C and C≡N carbons in the spectra of anion-π complexes as compared to the individual TCNE (Figure S12

in the Supporting Information). The measurements were further complicated by the substantial broadening of these signals in the presence of anions (up to their complete disappearance in the presence of bromide) which hindered quantitative measurements of complex formation using this method.

Computations. Geometries of the complexes were optimized without constraints via M06-2X/def2-TZVPP calculations (with ultrafinegrid option) using the Gaussian 09 suite of programs.[47-49] The absence of imaginary frequencies confirmed that the optimized structures represent true minima. Calculations with dichloromethane as the medium were done using a polarizable continuum model.[50] An earlier analysis demonstrated that intermolecular associations are well-modelled using this method.[17,37, 51, 52] The def2-TZVPP basis set does not include a diffuse function since previous analysis demonstrated that very similar results were obtained in the modelling of noncovalent interactions involving anions with the triple-ζ basis sets with and without diffuse functions.[53] Binding energies, ΔE were determined as: $\Delta E_b = E_C - (E_A + E_X)$, where E_C, E_A, and E_X are sums of the electronic energy and zero-point energy (ZPE) of the optimized complex, TCNE and anion, respectively. The energies of the optimized complexes and their components are listed in Table S8 in the Supporting Information. The UV-Vis spectra were obtained via TD-DFT calculations of the complexes and their components optimized in the corresponding solvent. QTAIM[31] and NCI[34] analyses of the solid-state associations and optimized complexes were performed using the atomic coordinates extracted from the X-ray structures with Multiwfn and visualized using VMD programs.[54,55] (The NCI setting was: isovalue = 0.5, color-coded with sgn(λ2)ρ in the range from −0.04 a.u. (blue, strong attractive interaction) to 0.02 a.u. (red, strong nonbonded overlap). Energy decomposition analyses (EDA) were carried out using the Amsterdam density functional (ADF) of the Amsterdam Modelling Suite[40, 41] via single-point calculations with the B3LYP-D3 functional (since it allowed evaluation of the dispersion component of the interaction energy) and the TZ2P basis set available in AMS using atomic coordinates of the complexes optimized as described above.

Conclusions

The positive electrostatic potential over the face of TCNE suggests that anions are attracted to this π-acceptor. However, whereas the interaction of TCNE with non-coordinating inert anions ClO_4^-, BF_4^-, and PF_6^- led to formations of the persistent anion-π complexes, the kinetic stability of the other anion-π associations under study were delimited by the oxidation potentials and nucleophilicity of the anions (Scheme 1).

Scheme 1. Persistent vs transient anion-π complexes of TCNE.#

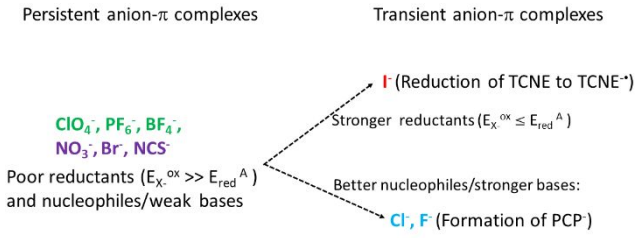

In particular, the values of E^o for $X^{\bullet}/X^-$ pair of 3.06, 2.03, 1.60 and 1.06 V vs SCE for X = F, Cl, Br and I, respectively, are higher than that for TCNE/$TCNE^{\bullet-}$ (E^o = 0.17 V).[17] The redox-potentials for the I_3^-/I^- pair, however, is 0.06 V,[35] which explains facile reduction of TCNE to $TCNE^{\bullet-}$ by I^- (eq. 2) and similar reduction of tetrahalosubstituted p-benzoquinones which we reported earlier.[17] As such, the transient appearance of the anion-π complexes upon mixing TCNE with iodide is followed by the fast formation of the $TCNE^{-\bullet}$ anion-radicals .

The oxidation potentials of the other anions considered in the current work are higher than that of reduction potential of TCNE. As such, they are not capable of efficient reduction of this π-acceptor. (For example, redox-potential of the Br_3^-/Br^- pairs is 0.39 V vs SCE. Thus, while bromide reduces dichlorodicyano-p-benzoquinone, DDQ (E = 0.52 V for DDQ/$DDQ^{\bullet-}$ pair),[17] the rate of reduction of TCNE by this anion is very small, if any.) However, the basicity and nucleophilicity of halide anions in aprotic solvents is increasing from I^- to Br, Cl^- and F^-.[36] The interaction of TCNE with better nucleophiles and stronger basis, e.g. Cl^- or F^-, led to chemical transformations producing PCP^- anions (similar to that described previously in solutions containing basis and water[29,30]), and only transient anion-π complexes were observed in the solutions of TCNE and Cl^- anions. Thus, among halide anions, only bromide (which is weaker reducing agent as compared to iodide, and weaker base/nucleophile than chloride or fluoride) formed rather persistent anion-π associations with TCNE.#

It is also important to note, that thermodynamics, UV-Vis spectral, and structural features of the anion-π complexes of TCNE are closely related to the corresponding complexes of analogous anions with aromatic (such as tetracyanopyrazine) and p-benzoquinone (such as tetrafluoro-p-benzoquinone) acceptors. Furthermore, energy-decomposition analysis demonstrated that variations of the contributions of E_{elstat}, ΔE_{oi}, and ΔE_{disp} in complexes of TCNE with various anions (and also distinctions in the spectral properties of the corresponding complexes) are similar to those which were found for the complexes of the same anions with aromatic and p-benzoquinone π-acceptors. This underlines the critical role of the nature of the anions in these bindings. It also points towards a general equivalence of the interactions of anions with TCNE with those established earlier with aromatic molecules and p-benzoquinones. As such, it extends a realm of the fascinating anion-π interactions from the systems involving electron deficient arenes and quinones to the alkene π-acceptors.

Overall, this work i) established the facile formation of anion-π complexes with TCNE and the conditions of the interchange between the persistent associations and transient complexes leading to redox or nucleophilic addition reactions, and ii) demonstrated that characteristics of such complexes of this olefinic π-acceptor are closely related to those of the reported electron-deficient aromatic and *p*-benzoqiuinone molecules.

Author Contributions

Conceptualization and methodology, S.V.R.; X-ray analysis, M. Z., UV-Vis measurements and crystallization , F.E.O. and S.M.; compu-

tations, F. E. O. and S.V. R.; data curation, F.E.O., S.M., M.Z., S.V.R.; writing—original draft preparation, S.V.R.; writing—review and editing, F.E.O., S.M., M.Z., S.V.R.; visualization, supervision, project administration, funding acquisition, S.V.R. All authors have read and agreed to the published version of the manuscript.

Conflicts of interest

There are no conflicts to declare.

Acknowledgements

We thank the National Science Foundation (grant CHE-2003603) for the financial support of this work. Calculations were done on Ball State University's beowulf cluster, which is supported by the National Science Foundation (MRI-1726017) and Ball State University. X-ray measurements were supported by the National Science Foundation through the Major Research Instrumentation Program under Grant No. CHE 1625543 (funding for the single crystal X-ray diffractometer).

Notes and references

‡ The PCP^- anions were previously synthesized by the reaction of TCNE with water in the presence of a base (which formed a σ-bonded intermediate with the π-acceptor).[29,30] Also, computational analyses in the previous studies[17] and in the current work indicated that F^- anions form the σ-bonded intermediates with the π-acceptors which explains the formation of PCP^- in the presence of these nucleophilic anions. To the best of our knowledge, however, σ-complexes with Cl^- anions were not reported and the computations of TCNE·Cl^- pairs in the current work produced anion-π complexes as the most stable structure. Yet, the location of chloride in these complexes was well suited for the nucleophilic attack on the sp^2 carbon. Furthermore, while the Cl…C distance in such complexes optimized in CH_2Cl_2 was 2.694 Å, calculations in the gas phase produced association with the Cl…C distance of 2.142 Å (and the essentially tetrahedral geometry of the carbon). The detailed analysis of the mechanism of the formation of PCP^- requires, however, a separate study and it is beyond the scope of the current work, which is focused on the nature of the anion-π complexes of TCNE with various anions.

§ The energies of the absorption bands obtained from the TD DFT calculations were 3.18 eV, 2.68 eV, and 2.21 eV, for anion-π complexes of TCNE with Cl^-, Br^-, and I^- anions, respectively (as compared to the measured values of 3.04 eV, 2.65 and 1.91 eV of the persistent or transient bands measured in the solution of TCNE with these anions). The calculated absorption band energy of PCP^- anion was 3.54 eV as compared to the energy of 4.12 eV of the absorption band formed at λ = 301 nm upon the addition of chloride to the solution of TCNE.

Note that anion-π complexes of TCNE with Br^-, NCS^- and NO_3^- anions were sufficiently persistent for the measurements of the complex formation in solutions and for the preparation of their single crystal for the X-ray structural measurements (see Methods for details). However while these crystalline anion-π associations could be stored for several weeks in the refrigerator, the decomposition of the anion-π complexes of TCNE with these anions was observed in solution at room temperature (see Figure S10 in the Supporting Information. Spectral changes suggest that these reactions led to formation of small amount of anion-radial of TCNE and/or PCP^- and these processes were faster in more polar acetonitrile than in dichloromethane. However, the detailed analysis of kinetics and mechanism of these processes requires a separate study and is beyond the scope of the current work.

1 D. Quinonero, C. Garau, C. Rotger, A. Frontera, P. Ballester, A. Costa and P. M. Deya, *Angew. Chem., Int. Ed.*, 2002, **41**, 3389.
2 I. Alkorta, I. Rozas and J. Elguero, *J. Am. Chem. Soc.*, 2002, **124**, 8593.
3 Mascal, A. Armstrong and M. D. Bartberger, *J. Am. Chem. Soc.*, 2002, **124**, 6274.
4 (a) A. Frontera, P. Gamez, M. Mascal, T. J. Mooibroek and J. Reedijk, *Angew. Chem., Int. Ed.,* **2011**, *50*, 9564. (b) A. Bauzá, T. J. Mooibroek and A. Frontera, *ChemPhysChem*, 2015, **16**, 2496.
5 B. L. Schottel, H. T. Chifotides and K. R. Dunbar, *Chem. Soc. Rev.*, 2008, **37**, 68.
6 (a) M. Giese, M. Albrecht and K. Rissanen, *Chem. Commun.*, 2016, **52**, 1778. (b) M. Giese, M. Albrecht and K. Rissanen, *Chem. Rev.* 2015, **115**, 8867. (c) S. V. Rosokha, *ChemPlusChem,* 2023**, 88**, e202300350.
7 G. Gil-Ramírez, E. C. Escudero-Adán, J. Benet-Buchholz and P. Ballester, *Angew. Chem., Int. Ed.,* 2008, **47**, 4114.
8 S. Demeshko, S. Dechert and F Meyer, *J. Am. Chem. Soc.*, 2004, **126***,* 4508.
9 Y. S. Rosokha, S. V. Lindeman, S. V. Rosokha and J. K. Kochi, *Angew. Chem., Int. Ed.*, 2004, **43**, 4650.
10 (a) O. B. Berryman, V. S. Bryantsev, D. P. Stay, D. W. Johnson and B. P. Hay, *J. Am. Chem. Soc.*, 2007, **129**, 48. (b) D.-X. Wang and M.-X. Wang, *J. Am. Chem. Soc.*, 2013, **135**, 892.
11 P. Ballester, *Acc. Chem. Res.*, 2013, **46**, 874.
12 (a) D.-X. Wang and M.-X. Wang, *Acc. Chem. Res.,* 2020, **53**, 1364. (b) H. Wang, W. Wang and W. J. Jin, *Chem. Rev.,* 2016, **116**, 5072.
13 Y. Zhao, Y. Cotelle, L. Liu, J. López-Andarias, A. B. Bornhof, M. Akamatsu, N. Sakai and S. Matile, *Acc. Chem. Res.*, 2018, **51**, 2255.
14 D. Quinonero, A. Frontera and P. M. Deya, Anion-π interactions in molecular recognition. In *Anion Coordination Chemistry*, K. Bowman-James, A. Bianchi, E. Garcia-Espana, Eds. 2012, 321.
15 J. Mareda and S. Matile. *Chem. Eur. J.,* 2009, **15**, 28.
16 E. Kuzniak, J. Hooper, M. Srebro-Hooper, J. Kobytarczyk, M. Dziurka, B. Musielak, D. Pinkowicz, J. Raya, S. Fertay and R. A. Podgajny, *Inorg. Chem. Front.,* 2020, **7**, 1851.
17 S. Kepler, M. Zeller and S. V. Rosokha, *J. Am. Chem. Soc.*, 2019, **141**, 9338.
18 (a) K. Molčanov, G. Mali, J. Grdadolnik, J. Stare, V. Stilinović and B. Kojić-Prodić, *Cryst. Grow. Des.*, 2018, **18**, 5182. (b) V. Milasinovic, V. Vukovic, A. Krawczuk, K. Molcanov, C. Hennig andM. Bodensteiner, M. *IUCrJ,* 2023, **10**, 156.
19 R. W. Newberry, R. T. Raines, *Acc. Chem. Res.,* 2017**, 50**, 1838.
20 B. Han, J. J. Lu and J. K. Kochi, *Cryst. Grow. Des.*, 2008, **8**, 1327.
21 J. Wilson, T. Maxson, I. Wright, M. Zeller, S. V. Rosokha, *Dalton Trans.,* 2020, **49**, 8734.
22 T. Cairns, R. Carboni, D. Coffman, V. Engelhardt, R. Heckert, E. Little, E. Mcgeer, B. Mckusick, W. Middleton, R. Scribner, C. Theobald and H. Winberg, *J. Am. Chem. Soc.,* 1958, **80**, 2775.
23 F.E. Odubo, M. Zeller and S. Rosokha *J. Phys. Chem. A*, 2023, **127**, 5851.
24 S. V. Rosokha and J. K. Kochi, *Acc. Chem. Res.,* 2008, **41**, 641.
25 (a) O. Webster, W. Mahler and R. Benson, *J. Am. Chem. Soc.,* 1962, **84**, 3678. (b) D. N. Dhar, *Chem. Rev.,* 1967, **67**, 611.
26 (a) A. Zheludev, A. Grand, E. Ressouche, J. Schweizer, B. G. Morin, A. J. Epstein, D. A. Dixon and J. S. Miller*, J. Am. Chem. Soc.,* 1994, **116,** 7243. (b) J.-M. Lu, S. V. Rosokha and J. K. Kochi, *J. Am. Chem. Soc.* 2003, **125,** 12161.
27 S. V. Rosokha, M. D. Newton, M. Head-Gordon and J. K. Kochi, *Chem. Phys.,* 2006, **324**, 117.
28 (a) J. S. Miller and A. J. Epstein, *Chem. Commun.,* 1998, 1319.

(b) J.S. Miller, *Chem. – Eur. J.,* 2015, **21**, 9302.
29 W. Middleton, R. Heckert, E. Little and C. Krespan, *J. Am. Chem. Soc.,* 1958, **80**, 2783.
30 Z. Rappoport, *J. Chem. Soc.,* 1963, 4498.
31 R. F. W. Bader, *Chem. Rev.,* 1991, **91**, 893.
32 E. Espinosa, E. Molins and C. Lecomte, *Chem. Phys. Lett.,* 1998, **285**, 170.
33 Popelier, P. L. A. The QTAIM perspective of chemical bonding in *The Chemical Bond*, John Wiley & Sons, Ltd, 2014, p. 271.
34 E. R. Johnson, S. Keinan, P. Mori-Sánchez, J. Contreras-García, A. J. Cohen and W. Yang, *J. Am. Chem. Soc.*, 2010, **132**, 6498.
35 J. Datta, A. Bhattacharya and K. K. Kundu, *Bull. Chem. Soc. Jpn.,* 1988, **61**, 1735.
36 M.B. Smith, March's Advanced Organic Chemistry: Reactions, Mechanisms, and Structure 8th Ed. Wiley, Hobolken, New Jersey, 2020.
37 R. S. Mulliken and W. B. Person, Molecular Complexes, Wiley: New York, 1969.
38 D. Howe, J. Wilson and S. V. Rosokha, *J. Phys. Chem. A*, 2022, **126**, 4255.
39 (a) H. B. Burgi, *Inorg. Chem.,* 1973**, 12**, 2321. (b) H. B. Burgi, J. D. Dunitz, J. M. Lehn and G. Wipff, *Tetrahedron,* 1974**, 30**, 1563. (c) H. B. Burgi, J.D. Dunitz and E. Shefter, *J. Am. Chem. Soc.,* 1973**, 95**, 5065.
40 E. J. Baerends, T. Ziegler, J. Autschbach, D. Bashford, A. Berger, A. Bérces, F. M. Bickelhaupt, C. Bo, P. L. de Boeij, P. M. Boerrigter and S. Borini,et.al. ADF2012.01; SCM: Amsterdam, 2012.
41 (a) F. M. Bickelhaupt and E. J. Baerends,. Kohn-Sham density functional theory: predicting and understanding chemistry. In *Reviews in Computational Chemistry*; John Wiley & Sons, Ltd, 2000; 1. (b) G. te Velde, F. M. Bickelhaupt, E. Baerends, C. Fonseca Guerra, S. J. A. van Gisbergen, J. G.; Snijders and T. Ziegler, *J. Comput. Chem.,* 2001, **22**, 931.
42 E. V. Anslyn and D. A. Dougherty, Univ. Sci. Books, Sausalito, California, 2006, p. 186.
43 *Bruker Apex3 v2016.9-0, SAINT V8.37A,* Bruker AXS Inc.: Madison, WI, 2016.
44 (a) Sheldrick, G. *SHELXTL suite of programs,* Version 6.14, 2000-2003, Bruker AXS Inc.: Madison, WI, 2003. (b) G. M. Sheldrick, Acta Cryst. A64, 2008, 112.
45 G.M. Sheldrick, *Acta Cryst*. A71 2015, 3.
46 C. Hübschle, G. Sheldrick and B. Dittrich, *J. Appl. Crystallogr.,* 2011, **44**, 1281.
47 Gaussian 09, Revision C.01, M. J. Frisch, G. W. Trucks, H. B. Schlegel, G. E. Scuseria, M. A. Robb, J. R. Cheeseman, G. Scalmani, V. Barone, B. Mennucci, G. A. Petersson, H. Nakatsuji, M. Caricato, X. Li, H. P. Hratchian, A. F. Izmaylov, J. Bloino, G. Zheng, J. L. Sonnenberg, M. Hada, M. Ehara, K. Toyota, R. Fukuda, J. Hasegawa, M. Ishida, T. Nakajima, Y. Honda, O. Kitao, H. Nakai, T. Vreven, J. A. Montgomery, Jr., J. E. Peralta, F. Ogliaro, M. Bearpark, J. J. Heyd, E. Brothers, K. N. Kudin, V. N. Staroverov, R. Kobayashi, J. Normand, K. Raghavachari, A. Rendell, J. C. Burant, S. S. Iyengar, J. Tomasi, M. Cossi, N. Rega, J. M. Millam, M. Klene, J. E. Knox, J. B. Cross, V. Bakken, C. Adamo, J. Jaramillo, R. Gomperts, R. E. Stratmann, O. Yazyev, A. J. Austin, R. Cammi, C. Pomelli, J. W. Ochterski, R. L. Martin, K. Morokuma, V. G. Zakrzewski, G. A. Voth, P. Salvador, J. J. Dannenberg, S. Dapprich, A. D. Daniels, O. Farkas, J. B. Foresman, J. V. Ortiz, J. Cioslowski and D. J. Fox, Gaussian, Inc., Wallingford CT, 2009.
48 Y. Zhao and D. G. Truhlar, *Theor. Chem. Acc.*, 2008**, 120,** 215-41.
49 F. Weigend and R. Ahlrichs, *Phys. Chem. Chem. Phys*., 2005**, 7**, 3297.
50 J. Tomasi, B. Mennucci and R. Cammi, *Chem. Rev.*, 2005, **105**, 2999–3093.
51 Z. Zhu, Z. Xu and W. Zhu, *J. Chem. Inf. Model*., 2020, **60**, 2683.
52 K. Wang, J. Lv and J. Miao, *Theor. Chem. Acc.,* 2015, **134**, 5.
53 A. Bauzá, D. Quiñonero, P. M. Deyà and A. Frontera, *J. Phys. Chem. A,* 2013, **117**, 2651.
54 T. Lu and F. Chen, *J. Comput. Chem.*, 2012, **33**, 580.
55 W. Humphrey, A. Dalke and K. Schulten, *J. Mol. Graphics*, 1996, **14**, 33.

The data supporting this article have been included as part of the Supplementary Information. Crystallographic data for $(Pr_4N)NO_3$□TCNE, $(Pr_4N)PF_6$□TCNE, $((Pr_4N)ClO_4)_2$□TCNE, $(Pr_4N)BF_4$□TCNE, and $(MePh_3N)Br$□TCNE and Bu_4NPCP (where PCP = 1,1,2,3,3-pentacyanoprop-2-en-1-ide) has been deposited at the Cambridge Crystallographic Data Centre under 2353176-2353181 and can be obtained free of charge via www.ccdc.cam.ac.uk/data_request/cif . .